Octatetraene Photoisomerization

Bryan E. Kohler

Department of Chemistry, University of California, Riverside, California 92521-0403

Received August 5, 1992 (Revised Manuscript Received November 11, 1992)

Contents

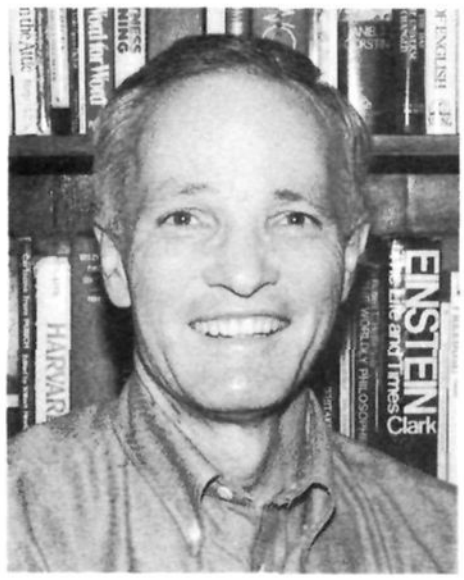

Bryan E. Kohler was born in Heber City, UT, June 9, 1940. He received a B.A. from the University of Utah in 1962 and a Ph.D. from the University of Chicago in 1967, under the guidance of Prof. Clyde A. Whitaker, Jr. He was a postdoctoral fellow with Prof. C. A. Hutchison, Jr., at the University of Chicago (1967) and with Prof. G. Wilse Robinson at California Institute of Technology (1968). Prof. Kohler has been an Assistant Professor and Associate Professor at Harvard University (1969–1975), an Associate Professor and Professor at Wesleyan University (1975–1985), and a Professor at the University of California, Riverside since 1985. He has been a Guest Professor at the University of Lieden (Kamerlingh Onnes Laboratory with John H. van der Waals, 1973) and at the Physikalische Institut, Universität Bayreuth (1984–1985). His honors include being an Enrico Fermi Research Fellow (1967), a NSF Postdoctoral Fellow (1968), an Alfred P. Sloan Foundation Fellow (1974), a Visiting Fellow, Joint Laboratory for Laboratory Astrophysics (1978 and 1991), an Alexander von Humboldt Fellow (1979), a Fellow of the American Physical Society, and a Guggenheim Fellow (1984–1985). He is a member of Sigma Xi, American Physical Society, New York Academy of Science, Biophysical Society, American Chemical Society, American Society for Photobiology, the Connecticut Academy of Arts and Sciences, and Oroborus.

I. Introduction

The photochemistry of rhodopsin and bacteriorhodopsin has taught us that linear polyenes can efficiently photoisomerize, even when they are enclosed in well-defined molecular cavities.[1] The fact that there is considerable selectivity in binding the polyene chromophores in these systems suggests that, especially on the time scales of electronic excitation, the molecular environment in these biopolymers is relatively rigid. That is, much more like the environment in an organic solid than the environment in a low molecular weight organic liquid. Since there is considerable support for the idea that a viscous solvent should suppress photoisomerization, it becomes especially important to go into the question of mechanism in this case, that is, to delineate the key features of the ground- and excited-state potential energy surfaces that determine the photoisomerization behavior of linear polyenes in molecular cavities.

Octatetraene in *n*-alkane solid solution is an excellent model for the photochemical behavior of the more complex visual and bacteriorhodopsin pigments. It is another system where a mid-sized linear polyene in a well-defined molecular cavity can be photoisomerized but where, in contrast to situation for the more complex biological systems, vibrationally resolved optical spectra can be measured. The ability to study photoisomerization under exactly the same conditions as those that are required for high information content spectroscopic investigations raises a special opportunity to work out the microscopic mechanism. In the particular case of low-temperature *n*-alkane solutions of octatetraene, vibrationally resolved optical spectra have been measured for all three double bond isomers and enough additional information on the dynamics and photoisomerization behaviors of these species has been accumulated to allow the identification of the key elements of this mechanism. The aim of this paper is to review these data and to communicate how they fit into a general model for linear polyene photoisomerization.

0009-2665/93/0793-0041$12.00/0

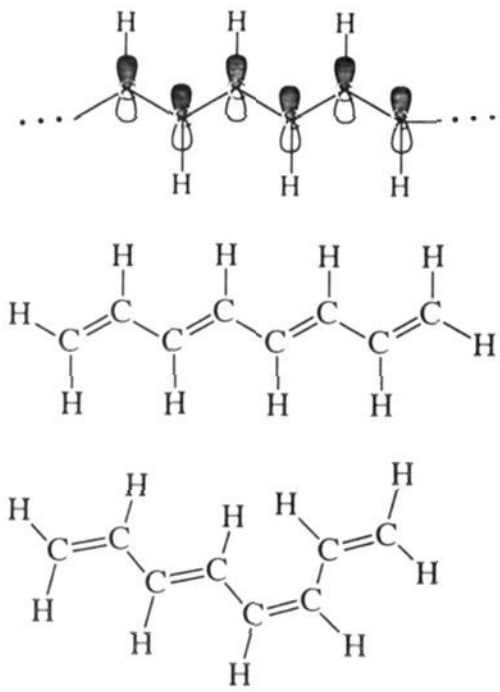

Figure 1. Conjugated linear chains. At the top is sketched the sp^2 hybridized chain with the $2p\pi$ atomic orbitals on which the delocalized π-molecular orbitals are based. Below this are shown the valence bond representations of two isomers of octatetraene (trans,trans, middle and cis,trans, bottom).

The rest of this paper has two main parts. In Section II the present understanding of linear polyene electronic structure with particular emphasis on the S_1 and S_2 states is reviewed. Then in Section III important aspects of linear polyene photochemical and photophysical behavior that have to be accounted for in any photoisomerization mechanism are reviewed and the microscopic model that we feel most consistently accounts for the available data is described.

II. Linear Polyene Electronic Structure

A. Molecular Geometry

Our discussion of electronic structure starts with the conjugated polyene backbone. It is the delocalization of π-electrons along this backbone that gives polyenes their characteristic optical spectra. Moreover, these delocalized π-electrons are largely responsible for the photophysical and photochemical responses of these *molecules including cis–trans photoisomerization.*

The formula for an unsubstituted polyene hydrocarbon is $C_{2n}H_{2n+2}$ where n is the number of formal double bonds. As shown in Figure 1, the carbon atoms are arranged in a planar zig-zag chain and the formal repeat unit, —CH=CH—, is an ethylene molecule. As the bonding representation sketched in Figure 1 implies, there is pronounced bond-length alternation. The length of a formal single bond (1.45 Å)[2] is shorter than the C–C bond in a normal alkane (1.53 Å)[3] although the length of a formal double bond (1.34 Å)[2] is the same as the C=C bond length in ethylene (1.336 Å).[4] The C=C—C bond angles in the linear polyenes are all very close to 125°. The shortening of the single bonds is consistent with the idea that the π-electrons are delocalized; that is, they are able to move up and down the polyene chain. In the ground state the barriers to rotation about the formal double bonds are high enough (20–40 kcal/mol) that double bond cis and trans isomers exist as independent, distinct molecules. The barrier to rotation about formal single bonds is sufficiently low (ca. 4 kcal/mol)[5] that these species rapidly interconvert in room-temperature solution although they may be studied as independent species at low temperature.[5–7]

B. Photochemically Relevant Excited States

The most fundamental description of a unimolecular photochemical mechanism would consist of detailing the potential energy surface (plot of electronic energy versus nuclear configuration) for the photochemically active state and identifying the primary path on this surface that leads from reactant to product. Thus, a discussion of photochemical mechanism properly begins with the question "What is the photochemically relevant state?".

A large body of empirical evidence argues that, in the case of linear polyene photoisomerization, the answer to this question is that photochemistry is initiated in S_1, the lowest energy excited singlet state. The idea that in the condensed phase vibrational relaxation and internal conversion within a given spin manifold are much faster than the rate of photochemical transformation[8] is so generally accepted that it is now referred to as "Kasha's rule". Lacking evidence for violation of Kasha's rule and given that, at least for the polyene hydrocarbons, internal conversion to the triplet manifold can be neglected,[9] the conclusion that linear polyene photoisomerization originates in the S_1 state follows.

In 1972 Hudson and Kohler reported high-resolution optical spectra that showed that the excited state responsible for the longest wavelength strong absorption band in diphenyloctatetraene was not the lowest energy excited singlet state.[10] Since this contradicted very general predictions of molecular orbital theory at the Hartree–Fock level, this was a startling finding. In an accompanying publication Karplus and Schulten[11] showed that explicit consideration of electron–electron correlation (through configuration interaction including double excitations from the ground state in their calculations) was essential if the theoretically predicted state ordering was to agree with experiment. Even though there had been previous suggestions that electron–electron correlation could be important in π-electron systems,[12,13] no one had predicted that it would be so important as to rearrange the predicted ordering of excited singlet states in the polyene hydrocarbons. Because the presence of a previously undetected excited singlet state at lower energy rationalized general polyene fluorescence properties that had been thought to be anomalous (Figure 2), it was conjectured that all linear polyenes would have a similar "hidden" low-lying excited singlet state.[14] We now know that this is true. For the purposes of this review it is useful to review the experimental grounding of the present interpretation of polyene optical absorption and emission spectra and to describe the relatively newly discovered S_1 state in terms of simple molecular orbital concepts. The present picture of linear polyene electronic structure represents a major paradigm shift from what is presented in much of the classical literature of physical organic chemistry. For this reason, it is presented at a level of detail that will be redundant for many readers who are invited to skip directly to section III. This presentation is also hueristic, aiming at communicating physical concepts and simple models rather than reviewing the current state of theoretical

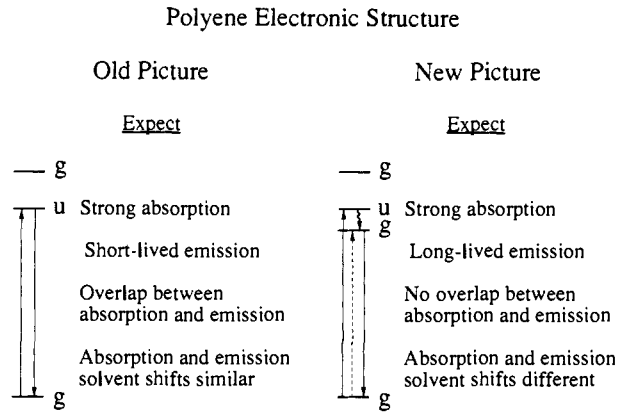

Figure 2. Energy level diagrams for linear polyenes before and after 1972.

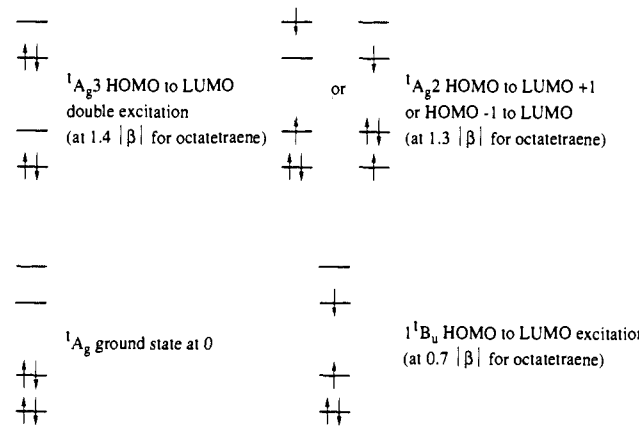

Figure 3. Orbital occupation for the most important linear polyene configurations.

treatments of linear polyene electronic structure (as has been done in a recent *Chemical Reviews* article[15]). A similar but even more elementary presentation of these ideas is found in a recent review of carotenoid electronic structure.[16]

Of course, understanding how the revised picture of excited-state ordering given in Figure 2 follows from vibrationally resolved UV/visible spectra does not require a microscopic picture of linear polyene electronic structure. However, such a picture is needed in order to appreciate what this revision in excited singlet state ordering means with respect to expected photochemical properties. Because it accounts for the excitation energy and intensity of the lowest energy strong absorption band of linear polyenes, the description of the π-electron states that comes out of Hückel theory can be considered to be extraordinarily successful. On the other hand, because Hückel theory incorrectly predicts that the excited state responsible for this absorption is S_1, the lowest energy excited singlet state (it is not S_1; it is S_2), Hückel theory may be considered to be fatally flawed. We will use it here for two reasons. First, almost everyone is conversant with LCAO-MO (linear combination of atomic orbitals–molecular orbital) theory at the Hückel level. Second, although the polyene S_1 state does not correspond to any single LCAO-MO configuration, it can be efficiently described in terms of linear combinations of just two Hückel configurations.

C. The Old Picture of Polyene Electronic Structure

In simple π-electron theory only the electrons not used in making the σ-bonded framework of sp^2 hybridized carbons are considered (refer to Figure 1). In the LCAO-MO approach the problem is to find the linear combinations of the atomic orbitals for these electrons (2p–π orbitals that are perpendicular to the plane of the zigzag chain) that are solutions of the Schrödinger equation for the polyene molecule. A linear polyene with n double bonds will have $2n$ 2p–π atomic orbitals which will lead to $2n$ linearly independent molecular orbitals. With the Hückel approximations for the molecular Schrödinger equation, this problem is sufficiently simple that it is routinely assigned to undergraduate students. The more enterprising of these quickly find that there is a closed form general solution for the molecular orbital energies and the atomic orbital coefficients for a given molecular orbital for a polyene with an arbitrary number of double bonds in conjugation.[17]

A configuration is a particular assignment of the $2n$ π-electrons to molecular orbitals. At this level of treatment, the energy of a given configuration is just the sum of the energies of the occupied molecular orbitals. It is common to associate molecular states with single configurations although, in the case of the linear polyenes, this leads to serious errors. The key configurations for understanding linear polyene electronic structure are introduced in Figure 3. In the minimum-energy or ground-state configuration (1^1A_g) all of the bonding molecular orbitals are doubly occupied. The lowest energy excited configuration (1^1B_u) is generated from the ground-state configuration by promoting one electron from the highest energy occupied molecular orbital (HOMO) to the lowest energy unoccupied molecular orbital (LUMO). Other single-electron promotions and multiple-electron promotions all lead to higher energy configurations, three of which are needed to describe the linear polyene S_1 state. For butadiene, which has four π-electron orbitals, the configurations are exactly those given in Figure 3. Analogous configurations obtain for all linear polyenes: each conjugated double bond beyond two just adds one doubly occupied bonding molecular orbital at the bottom and one empty antibonding molecular orbital at the top.

The agreement between Hückel theory and low-resolution spectra is excellent. With a proper choice of the energy of the Hückel resonance integral β, the predicted energy and transition intensity of the HOMO to LUMO excitation is close to the observations for the lowest energy strong absorption (1^1A_g to 1^1B_u) for a large number of compounds. If different resonance integrals are used for the formal single and double bonds, the correspondence between calculated and measured excitation energies can be made exact for the entire homologous series.[18]

While LCAO-MO theory provides a convincing interpretation of the low-resolution absorption spectra, aspects of the fluorescence spectra appear to be anomalous. As is apparent in the top panel of Figure 4, the fluorescence and absorption spectra have little overlap. This is most striking when there is some vibrational fine structure. As Figure 4 shows, in the case of octatetraene there is a gap of 3500 cm^{-1} between the lowest energy peak in the absorption spectrum and

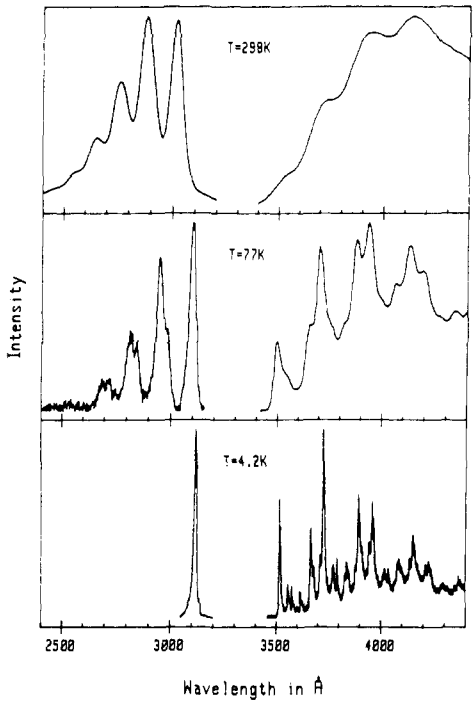

Figure 4. Absorption and fluorescence for an *n*-octane solution of *all-trans*-octatatetraene at different temperatures (room temperature at the top, 77 K in the center, and 4.2 K at the bottom). For each pair of spectra absorption is at the left, fluorescence at the right. As resolution is increased it becomes very clear that absorption and fluorescence involve different excited states.

the highest energy peak in the emission spectrum: if absorption and emission involved the same excited state, these peaks should coincide. Further, integration of the strong absorption band and application of the lifetime-intensity relation of Einstein as modified for polyatomic molecules by Strickler and Berg[19] leads to the prediction of a very short (1–2 ns) radiative lifetime. In fact fluorescence lifetimes are often much longer (173 ns for octatetraene in *n*-octane at 77 K[20]). Finally, the solvent shift behavior of the absorption and fluorescence spectra of a given molecule are different. The absorption shifts approximately 10^4 cm^{-1} to lower energy for unit change in $(\eta^2 - 1)/(\eta^2 + 2)$ where η is the refractive index for the solvent while changing solvent has little effect on the fluorescence.[14,21-23] All of these fluorescence anomalies suggested that there was a weakly absorbing excited state lower in energy than the 1^1B_u state, which was definitively established by high-resolution experiments like those described in the next section.

D. High-Resolution Experiments

The shapes of electronic absorption and fluorescence bands derive from the vibrational levels associated with the initial and final electronic states as is shown in cartoon form in Figure 5 (detailed discussions of vibrational fine structure in optical spectra can be found in standard texts[24]). Three kinds of inhomogeneity cause this vibrational fine structure to be almost completely washed out in spectra measured for room-temperature solutions. First, there is inhomogeneity of initial-state energy introduced by thermal population of excited vibrational levels in the ground state. Second, there is environmental inhomogeneity. The random

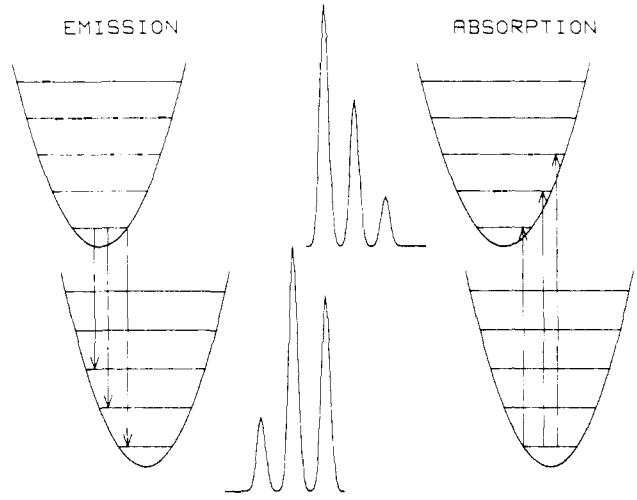

Figure 5. Vibrational fine structure in absorption and fluorescence spectra. Electronic energy as a function of conformation is the potential energy function for nuclear motion. As indicated, minimum-energy conformations are usually different in different electronic states. Absorption fine structure intervals (upper spectrum) are determined by excited state vibrational frequencies: emission fine structure intervals (lower spectrum) are determined by ground-state vibrational frequencies. The intensity of a fine structure component is proportional to the squared overlap of the ground- and excited-state vibrational functions.

structure in a liquid means that each solute molecule sees a different microenvironment and, thus, experiences a different solvent shift of its isolated molecule excitation energy. Third, for linear chain molecules like the polyenes, there is also inhomogeneity with respect to molecular conformation since at room temperature a number of s-cis conformers will be present. All of these sources of spectral broadening are significantly decreased by going to a low-temperature solid-state environment. Although this introduces some experimental complexity, the added information is well worth the effort. Vibrational resolution permits unambiguous and accurate determination of electronic excitation energies and gives detailed information on the potential energy surfaces that govern chemistry, including cis–trans isomerization.

To obtain vibrationally resolved spectra, the molecules under study must be in a low-temperature homogeneous environment. This may be accomplished in the condensed phase by growing dilute mixed crystals of the polyene in a transparent host and then cooling this mixed crystal to low temperature in a cryostat. In the gas phase where the molecular environment is already homogeneous (vacuum), the cooling can be realized by seeding the molecule under study into a supersonic rare gas expansion.[25] Although recent high-resolution gas-phase experiments indicate that free jet expansion techniques offer great promise for studying polyenes or carotenoids with up to 20 carbons,[7,26-31] we shall concentrate on the condensed-phase experiments.

The top part of Figure 4 shows the absorption spectrum measured for a room-temperature solution of the model polyene octatetraene in *n*-octane. Because of the simplicity of the molecule and the fact that the isomeric composition is more than 90% all-trans, the characteristic polyene absorption band already shows some vibrational fine structure. As is easily seen in the low-temperature spectra, most of the vibronic intensity involves the C=C and C—C stretch modes whose

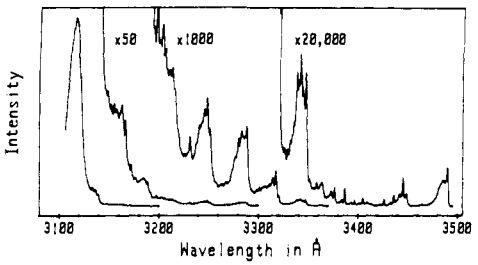

Figure 6. Absorption spectrum of an *n*-octane solution of octatetraene at increased sensitivity (achieved through fluorescence excitation techniques). This is just the spectrum shown in the lower left of Figure 4 replotted with successive scale magnifications.

frequencies are ca. 1600 and 1200 cm^{-1}, respectively. Because at room temperature the bands are broader than the difference between the C=C and C—C vibrational frequencies, these peaks are not resolved and an apparent spacing of ca. 1300 cm^{-1} is seen. As this solution is cooled to 77 K (liquid nitrogen), the *n*-octane becomes (poly)crystalline. The lower temperature and the fact that the molecular environment of the octatetraene guest molecules is now extremely homogeneous significantly increases the resolution of the absorption and fluorescence spectra as seen in the middle of Figure 4. Because of interference from light scattering, absorption measurements on polycrystalline samples are difficult to make. However, if samples fluoresce, the fluorescence excitation spectrum (fluorescence intensity vs the wavelength of the exciting light) which is just the absorption multiplied by the quantum yield for fluorescence is easily measured. If the attainment of Boltzmann equilibrium on the excited-state surface is fast compared to all other decay processes (true for linear polyenes in solution), then the quantum yield for fluorescence is independent of wavelength and the absorption and fluorescence excitation spectra are equivalent. To obtain a totally resolved spectrum, all that remains is to lower the temperature to 4.2 K (liquid helium). The resulting spectra are shown at the bottom of Figure 4.

The large gap between the absorption and emission spectra seen under high-resolution conditions clearly shows that they are associated with different excited states. The implication is that there is another extremely weakly absorbing excited state that lies lower in energy than the 1^1B_u state that is responsible for the strong absorption band. This weak absorption band may be directly seen by simply increasing sensitivity. Figure 6 shows the normal one-photon absorption (fluorescence excitation) spectrum of octatetraene in *n*-octane at increasingly high sensitivities. Since excitation of the weak features to the low-energy side of the strong absorption produces exactly the same high-resolution spectrum as that produced by exciting the strong band and photoselection experiments rule out energy transfer, both absorptions have to be assigned to the same molecule. Thus, high-resolution experiments definitively establish that there is a weakly absorbing excited state below the 1^1B_u state in octatetraene. Since all polyene π-electron states are either B_u or A_g, the weakness of the fluorescence excitation spectrum in Figure 6 and the strong increase in intensity as excitation energies approach the 1^1B_u origin suggests that this state is an A_g state. This assignment has been confirmed by two-photon excitation spectroscopy.[32]

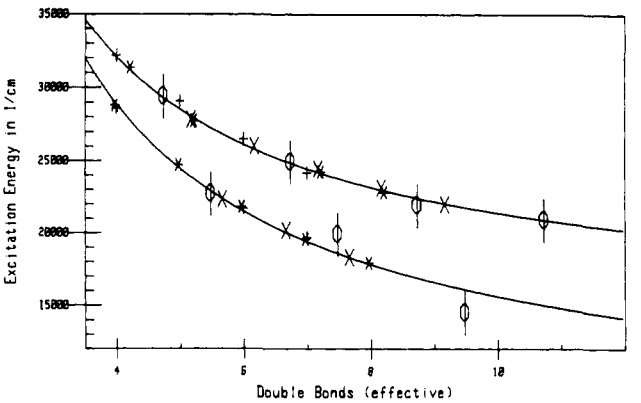

Figure 7. Universal curves for 2^1A_g and 1^1B_u excitation energies versus the effective number of conjugated double bonds. The line for 1^1B_u energy (upper curve) is $\bar{\nu} = 14\,250\ cm^{-1} + 71\,000\ cm^{-1}/n_{eff}$; the line for 2^1A_g energy (lower curve) is $\bar{\nu} = 6800\ cm^{-1} + 88300\ cm^{-1}/n_{eff}$. There are 18 experimental points on the upper curve: 9 plotted as * and I for unsubstituted and alkyl-substituted polyenes, respectively ($n_{eff} = n$), 5 plotted as + for diphenylpolyenes ($n_{eff} = n + 3.2$), and 4 plotted as ϕ for β-carotene oligomers ($n_{eff} = n - 0.3$). There are 14 experimental points on the lower curve: 8 plotted as * and I for unsubstituted and alkyl-substituted polyenes, respectively ($n_{eff} = n$), 3 plotted as + for diphenylpolyenes ($n_{eff} = n + 1.7$), and 3 plotted as ϕ for β-carotene oligomers ($n_{eff} = n + 0.5$).

Table I. Parameters for the Universal Curve $\bar{\nu} = A + B/n_{eff}$[a]

			$n_{eff} - n$		
	A (cm^{-1})	B (cm^{-1})	unsubstituted or α,ω-dialkyl	α,ω-diphenyl	α,ω-di-β-ionylidyl
2^1A_g	6800	88300	0	1.7	0.5
1^1B_u	14250	71200	0	3.2	−0.3

[a] n is the number of conjugated double bonds in the polyene chain.

1. Systematics of Linear Polyene S_1 and S_2 Energies

High-resolution condensed-phase optical spectra similar to those shown in Figures 4 and 6 have now been measured for a substantial number of linear polyenes[33] including unsubstituted linear polyenes with four through seven conjugated double bonds,[32,34-36] α,ω-dialkylpolyenes with three through eight double bonds,[37-41] and α,ω-diphenylpolyenes with four through six polyene double bonds.[42-44] In each homologous series the 2^1A_g and 1^1B_u excitation energies are well fit by the empirical relationship $\bar{\nu} = A + B/n$, where n is the number of conjugated double bonds. In a completely empirical treatment, different A and B parameters are needed for each excited state of each homologous series. A more satisfying the economical treatment is one where it is assumed that the effect of a given substituent is to change the conjugation length from n to $n_{eff} = n + \delta n_{substituent}$. With this formalism, the excitation energies of a number of different homologous series, including a series of β-carotene oligomers,[45] can be put onto the same universal curve as is seen in Figure 7. The parameters for this kind of empirical summary of linear polyene excitation energies are given in Table I.

The parameters in Table I allow the reliable estimation of the 2^1A_g and 1^1B_u 0–0 energies for *n*-alkane solutions of a wide variety of linear polyenes. It is also useful to be able to correct these estimates for the effects of solvent environment. Since the original analysis of the solvent shift behavior of diphenyloctatetraene

absorption and fluorescence spectra,[14] there have been a number of studies of the effect of solvent environment on 2^1A_g and 1^1B_u excitation energies.[21-23] To within a few hundred cm^{-1} the results of all of these studies may be summarized by saying that the 1^1B_u excitation energy obeys the relation $\bar{\nu} = \nu_0 + (\eta^2 - 1)/(\eta^2 + 2) \times 10^4$ cm^{-1}, where η is the solvent refractive index and that the 2^1A_g energy is nearly independent of solvent environment. The universal curves of Figure 7 and this simple estimate of the effects of solvent environment gives reasonable estimates for the S_1 and S_2 energies of an enormous variety of linear polyenes.

The high-resolution studies establish that, at least for polyenes with three through eight double bonds in conjugation, the inference made in Section II.B above is correct. That is, that under ordinary solution conditions the lowest energy intense absorption band of a polyene chromophore is associated with the $S_0 \rightarrow S_2$ transition and that the relaxed fluorescence comes from the $S_0 \leftarrow S_1$ transition. Thus, in those cases where relaxed fluorescence can be observed, estimates of the excitation energies of the S_1 and S_2 states can be extracted from the low-resolution spectra. Exceptions to this rule are expected to occur as the conjugated polyene chain becomes long and the energy separation between S_2 and S_2 approaches the energy separation between S_1 and S_0. The increased S_1–S_2 gap inhibits nonradiative relaxation from the S_2 state while the decreased S_1–S_0 gap enhances nonradiative decay of S_1. Because the intrinsic radiative rate of the symmetry allowed S_2 to S_0 transition is orders of magnitude larger than that of the symmetry forbidden S_1 to S_0 transition, even though the quantum yield for S_2 emission is extremely small ($<10^{-4}$), it can be seen. It now appears to be well established that the extremely feeble fluorescence that can be detected from solutions of β-carotene at 77 K[46] and room temperature[47] originates from S_2.

E. The New Picture of Polyene Electronic Structure

It is clear that the appealingly simple LCAO-MO model for linear polyene electronic structure is incompatible with the experimental observation that the state generated from the ground configuration by the promotion of a single electron from the HOMO to the LUMO is not the lowest energy excited singlet. The question of why this was the case (or what must be done to the theory to make it work) was raised and answered by Karplus and Schulten at the time of the first experiments.[11] They showed that the fundamental problem was the approximation that the interelectron repulsion energy could be treated by considering one electron interacting with an averaged charge cloud generated by all the rest. In other words, the π-electrons in linear polyenes move in such a highly correlated way as to invalidate one of the basic assumptions of molecular orbital theory. Explicit consideration of electron–electron interaction led to a strong mixing of the A_g symmetry configurations with the result that the mixture of the HOMO to LUMO doubly excited configuration with the antisymmetric combination of the HOMO $\rightarrow$ LUMO + 1 and HOMO − 1 $\rightarrow$ LUMO (see Figure 3) crossed below the 1^1B_u state. Rather than attempt a summary of the subsequent theoretical work, we refer the interested reader to recent reviews[15,48,49] and conclude this section with a description of a simple model that allows the estimation of 2^1A_g and 1^1B_u excitation energies in linear polyenes with any number of conjugated double bonds.

1. Simple Model for Calculating S_1 and S_2 Energies

Schulten and Karplus' demonstration that the correct order of polyene excited singlet states could only be obtained with explicit attention to electron–electron interaction has been reinforced by a number of subsequent theoretical studies.[50-53] Unfortunately, as theory more closely reflects experimental realities, it becomes less accessible to the nonexpert. The desire to have an interpretative theoretical model that could properly reproduce 2^1A_g and 1^1B_u excitation energies but that still had the mathematical simplicity and intuitive transparency of Hückel theory motivated us to ask the question, "What is the least that would have to be done to the Hückel model to make it work?". It turns out that by solving a quadratic equation involving two Hückel energies and a chain length dependent mixing parameter, all of the 25 2^1A_g and 1^1B_u excitation energies that have been obtained in high-resolution experiments can be reproduced with a root-mean-square deviation of only 160 cm^{-1}.[18] To communicate the essence of this model, we briefly review how it works for unsubstituted polyenes.

For unsubstituted polyene chains the energies of the configurations shown in Figure 3 are computed by Hückel theory using different resonance integrals for the single and double bonds, β_s and β_d, respectively. Our formulation expresses β_s and β_d in terms of the equal bond length resonance integral β and a bond alternation parameter ξ as $\beta_s = \beta e^{-\xi}$ and $\beta_d = \beta e^{+\xi}$ where $\beta = -30\,305$ cm^{-1} and $\xi = 0.1333$. The configurational energies are easily calculated using the simple and exact method published by Lennard-Jones in 1937.[54] For a chain containing N conjugated double bonds one first computes the N distinct values of θ_r that satisfy $\sin[(N+1)\theta_r] + \sin(N\theta_r)e^{-2\xi} = 0$, then computes the $2N$ orbital energies from $\epsilon = \pm\beta[2\cosh(\xi) + 2\cos(\theta_r)]$, and finally computes the energies of the four configurations shown in Figure 3 (the ground-state energy, the energy of the HOMO $\rightarrow$ LUMO excited state $E(1B_u)$, the energy of the HOMO − 1 $\rightarrow$ LUMO or HOMO $\rightarrow$ LUMO + 1 excited state $E(Ag2)$, and the energy of the excited state where two electrons are promoted from the HOMO to the LUMO $E(Ag3)$). Assuming that the Ag2 and Ag3 configurations are mixed by an off-diagonal element $P = A + B/N$, the final energy of the 2^1A_g state is given by $E(2^1A_g) = [E(Ag2) + E(Ag3)]/2 - (\{[E(Ag2) - E(Ag3)]/2\}^2 + P^2)^{1/2}$. For the unsubstituted polyenes $A = 12\,300$ cm^{-1} and $B = 58\,000$ cm^{-1}.

In a rigorous treatment of this simple model we would note that it is the antisymmetric linear combination of the degenerate HOMO − 1 $\rightarrow$ LUMO and HOMO $\rightarrow$ LUMO + 1 configurations that mixes with the HOMO $\rightarrow$ LUMO doubly excited configuration. While this has no consequences with respect to fitting excitation energies, it will be important in interpreting the P parameter, assigning higher lying A_g states, and calculating such off-diagonal properties as polarizability and 2-photon absorptivity (see, for example, recent comments on the "nA_g" state[55-57] and recent experiments

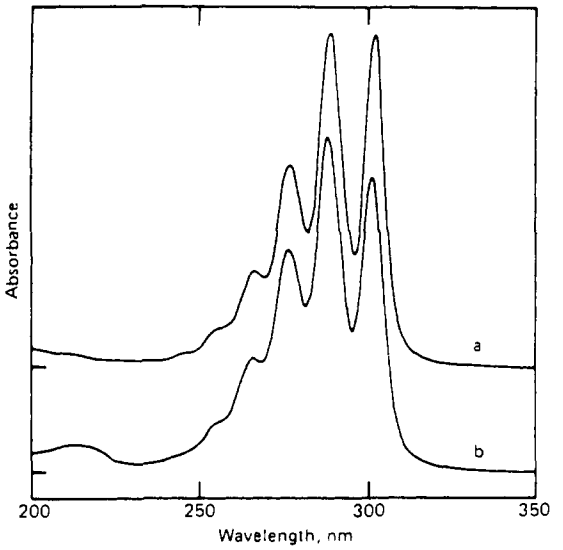

Figure 8. Room-temperature absorbance spectrum of *all-trans*-octatetraene (a) and *mono-cis*-octatetraene (b) in hexane. The spectra have been scaled to equal heights. The absorbance bands from 310 to 250 nm correspond to the $S_0 \rightarrow S_2$ ($1^1A_g \rightarrow 1^1B_u$) transition of a linear polyene of C_{2h} symmetry. The all-trans origin is at 302 nm and the mono-cis origin is at 301 nm.

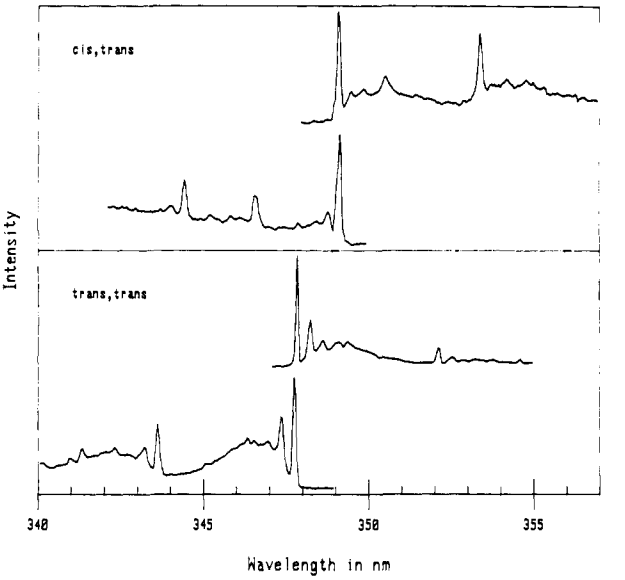

Figure 9. The 2^1A_g origin region of *cis,trans*-octatetraene (upper panel) and *trans,trans*-octatetraene (lower panel) in *n*-hexane at 4.2 K. Fluorescence goes to the right, fluorescence excitation to the left: the cis,trans 0–0 is at 349.0 nm and the trans,trans 0–0 is at 347.8 nm. In each case the formal symmetry is broken.

on β-carotene[47,58]). The reader is referred to the original literature for further details of this model[18] as well as for examples of its extension to substituted polyenes.[59,60]

III. Photochemistry

The optical spectra of room-temperature solutions of cis and trans isomers of a given linear polyene are quite similar because differences in the excitation energies of the different isomers is small compared to the widths of the spectroscopic bands. For example, Figure 8 compares the absorption spectrum of a room temperature *n*-hexane solution of *trans,trans*-octatetraene to that of the cis,trans isomer. Typically, shifts of band maxima of order 1 nm are observed. Although differences in the shape of the overall envelope of the spectra are more apparent (in general, optical spectra of the trans isomers have relatively more vibronic absorption intensity in the S_2 origin band than do cis isomers and cis isomers have relatively more intensity in a higher energy band at ca. 140 nm shorter wavelength), quite sophisticated data treatments are required to quantitatively decompose a measured spectrum into contributions from the different species.[61] For the very narrow bands that obtain for low-temperature *n*-alkane solutions of linear polyenes, the small differences in excitation energies of the cis and trans isomers are large compared to the band widths so that the spectra of cis and trans isomers are completely independent and easily distinguished as is seen in Figure 9.

Very soon after obtaining vibrationally resolved spectra for cis,trans octatetraene, we found, somewhat to our surprise, that even in these liquid helium temperature solid solutions the cis,trans and trans,-trans isomers could be photochemically interconverted.[62] This observation in and of itself immediately puts some very strong limits on possible mechanisms. These limits have been further narrowed by a variety of other experiments. The main task of this section is to summarize all of the experimental data that are relative to this low-temperature solid-state isomerization and to present a mechanism that is consistent with all that is presently known.

A. Low-Temperature Octatetraene Photochemistry

The photochemistry of low-temperature *n*-alkane solutions of octatetraene is surprisingly rich. So far, six distinguishable species have been identified and spectroscopically characterized in high-resolution experiments, and information on the photochemical and thermal processes by which they interconvert has been obtained. Since the original data are dispersed through papers whose primary focus was high-resolution spectroscopy, it is useful to briefly list the species and review what is known about them.

1. trans,trans-Octatetraene

First there is the trans,trans isomer. Under normal conditions, octatetraene solutions contain more than 90% of the trans,trans isomer: isomerically pure solutions are conveniently prepared by HPLC. Solutions prepared by these methods have been used to generate high-resolution reference spectra for the trans,-trans isomer in 4.2 K *n*-hexane, *n*-heptane, *n*-octane, *n*-nonane, and *n*-decane. The strict complementarity of the one-photon and two-photon spectra in *n*-octane[32] provides the strongest possible proof of identity since such spectra only obtain for strictly centrosymmetric molecules in strictly centrosymmetric environments. Exhaustive selective excitation studies show that, at least in *n*-hexane and *n*-octane, all of the prominent spectroscopic features belong to a single molecular species in a single site. It is clear that, as would be expected for a system that has been cooled through a succession of equilibrium states, the octatetraene molecule is not only trans about all double bonds but also trans about all single bonds as well.

2. cis,trans-Octatetraene

Stereoselective synthesis and HPLC purification allow the preparation of pure solutions of the cis,trans isomer which, in turn, allow the measurement of high-resolution reference spectra. Detailed studies have been made for *n*-hexane and *n*-octane hosts at 4.2 K.[63] Again, the low-temperature solutions contain a single species in a single molecular site. From the method of preparation we know that the octatetraene solute is cis,trans with respect to the distinguishable double bonds. From the fact that the S_2 (1^1B_u) excitation energy is not significantly red shifted with respect to that of the trans,trans isomer we know that there are no cis single bonds. It is significant that the spectrum of *cis,trans*-octatetraene produced by photolysing a 4.2 K solution of the trans,trans isomer is identical to the reference spectrum obtained by cooling a solution of the cis,trans isomer through a succession of equilibrium states.[64,65] Similarly, there is no difference between the high-resolution spectrum of photochemically generated *trans,trans*-octatetraene and the spectrum of a slowly cooled solution.[62,64]

3. cis,cis-Octatetraene

There are only three double bond isomers of octatetraene: trans,trans, cis,trans, and cis,cis. To fully investigate the low-temperature photochemistry of the octatetraene molecule, high-resolution spectroscopic characterization of all three species is needed. However, because of the efficiency with which *cis,cis*-octatetraene ring closes to cyclooctatriene, normal room-temperature synthetic and purification techniques cannot be used for sample preparation. The solution to the problem of sample preparation in this case was suggested by Data, Goldfarb, and Boikes who reported that photolysis of 1,3,5-cyclooctatriene in a low-temperature argon matrix resulted in the formation of several octatetraene isomers, one of which they argued was *cis,cis*-octatetraene.[66] Unfortunately, in their case unambiguous confirmation of the presence of the cis,-cis isomer was not possible because of the complexity of the sample. From this starting point we were able to develop a method for efficiently preparing *n*-alkane solutions of *cis,cis*-octatetraene and, by high-resolution spectroscopy and thermal studies, establish the molecular conformation.[67-69]

Fluorescence from 1,3,5-cyclooctatriene, even in low-temperature matrixes, is too weak to be detected by conventional techniques. However, 301-nm irradiation of a 10^{-3} M solution of cyclooctatriene in *n*-octane at 10 K generates a broad emission spectrum not unlike that seen for octatetraene in glassy solvents. Thermally cycling the sample from 10 K to 220 K to 10 K converts the broad emission spectrum into one that exhibits full vibrational resolution. Selective excitation shows that three species, all of which have the spectroscopic characteristics of octatetraene, are present. One of these is *cis,trans*-octatetraene. The other two have spectra that are virtually identical except for being slightly shifted with respect to each other (66 cm^{-1} for the fluorescence, 107 cm^{-1} for the fluorescence excitation). This establishes that these spectra belong to a single species present in two slightly different sites. The spectra associated with this species disappear after warming to 300 K and recooling to 10 K as would be expected for *cis,cis*-octatetraene. This assignment is confirmed by the fact that there is a gap between the origins of the 1-photon fluorescence excitation and fluorescence spectra for this species as is expected for a strictly symmetry forbidden transition. Two-photon fluorescence excitation studies confirm that both the ground and excited states of the photogenerated species in both sites are strictly centrosymmetric. The only possibility for a centrosymmetric thermally labile octatetraene is the cis,cis isomer. The two nearly but not exactly degenerate ways that *cis,cis*-octatetraene can be substituted for *n*-octane while satisfying the requirement of strict centrosymmetry of *both* molecule and environment are shown in Figure 10.

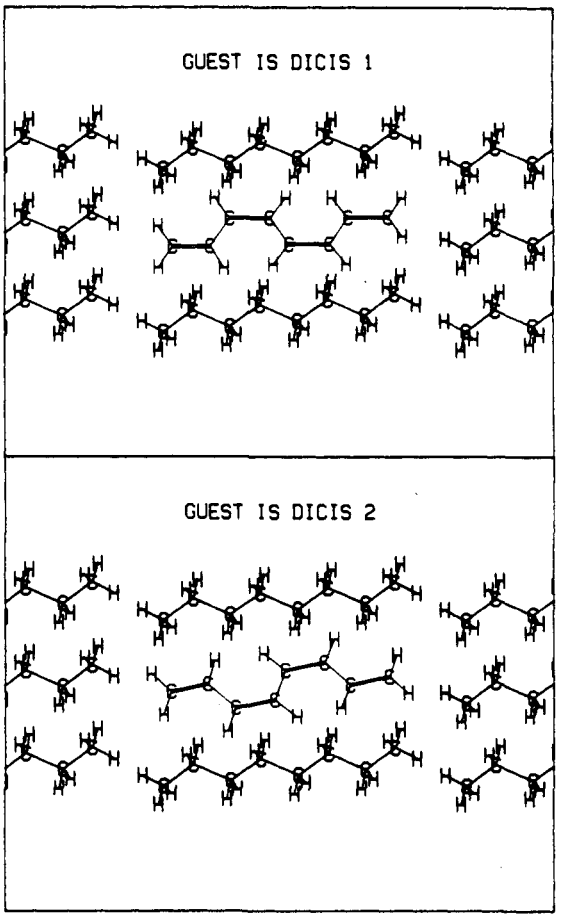

Figure 10. Proposed orientations of *di-cis*-octatetraene in the *n*-octane lattice for sites 1 and 2. The octatetraene guests have been placed substitutionally with the principal axes of the moment of inertia tensor aligned with those of the replaced *n*-octane molecule. This projection is the *bc* crystallographic plane of the *n*-octane crystal structure as reported by Mathisen and Norman (ref 3).

4. s-Cis

When a 4.2 K *n*-octane solution of *trans,trans*-octatetraene is irradiated at the S_1 origin, even at the low exciting light intensities that generate fluorescence spectra that can only be measured with photon-counting techniques, there is rapid accumulation of a photoproduct whose fluorescence and fluorescence excitation spectra are significantly red shifted. Spectroscopic characterization of this photoproduct[6] shows that it is a noncentrosymmetric molecule with S_1 and S_2 states that, except for a red shift (1360 cm^{-1} for S_1, 1750 cm^{-1}

for S_2), have the vibronic signature of octatetraene. When the sample is warmed to 50 K in the dark, this photoproduct reverts to the trans,trans precursor over a 4 kcal/mol barrier.[5] The only assignment consistent with these data is that the photoproduct is a single bond cis isomer. The size of the S_2 red shift (1250 cm^{-1} which is smaller than the 2900 cm^{-1} red shift reported for the butadiene 1^1B_u band maximum[70]) argues that there is only one s-cis linkage. While we feel that it is most likely 2-s-cis, the 4-s-cis conformation cannot be definitively ruled out.

5. Trans,trans (Site 2)

Extended irradiation of a 4.2 K solution of *trans, trans*-octatetraene in *n*-octane not only produces the cis,trans and s-cis isomers described above but yet another photoproduct whose high-resolution fluorescence and fluorescence excitation spectra are nearly identical to those of the trans,trans precursor. Although quantitative yield measurements have not been made, irradiation at the S_2 origin (312 nm) favors formation of the s-cis isomer while irradiation in the S_1 vibronic manifold (327.5 nm, 2120 cm^{-1} above the S_1 0–0 band) favors formation of the cis,trans isomer and this photoproduct.[64] Two-photon spectroscopy shows that this octatetraene product is rigorously centrosymmetric[71] and thermal studies show that it reverts to the trans,trans isomer in the thermodynamic site in the ground state over a very low barrier (0.6 kcal/mol).[65,71] These properties are only consistent with this photoproduct being the trans,trans isomer trapped in a nonequilibrium site. There are only two ways to substitute octatetraene for *n*-octane and preserve strict centrosymmetry of both the guest molecule and its environment. In one (the thermodynamic equilibrium site) the zig-zag pattern of the guest molecule matches that of the host molecule it replaces. In the other, the zig-zag pattern of the guest molecule is opposite to that of the host molecule that it replaces (see Figure 11). It is reasonable to postulate that *trans,trans*-octatetraene in this nonequilibrium site is generated by successive trans to cis and cis to trans photoisomerizations as shown in Figure 11. This idea receives support from the fact that the intensity of this photoproduct spectrum increases quadratically with the number of photons absorbed.[65]

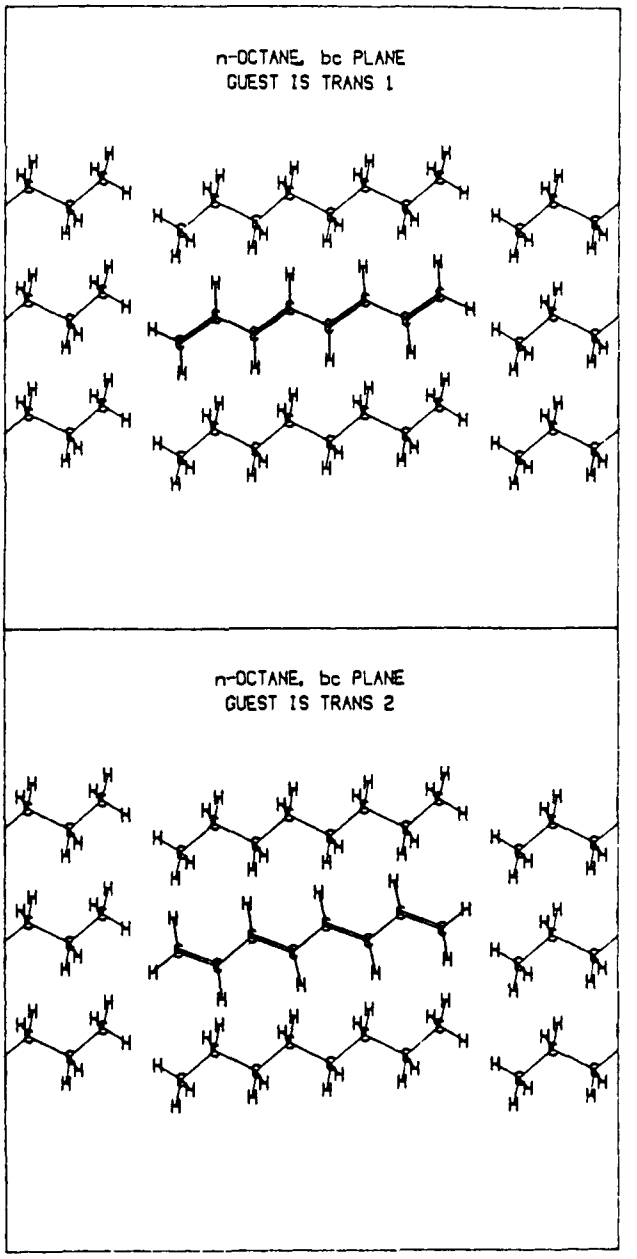

Figure 11. Proposed sites for *all-trans*-octatetraene in the *n*-octane lattice. The top frame shows the site assigned to initially prepared all-trans isomer (Trans1), and the site in the bottom frame is assigned to Trans2. This projection in the *bc* crystallographic plane of the *n*-octane crystal structure is reported by Norman and Mathisen (ref 3).

B. Mechanism for Low-Temperature Photochemistry

1. Spectroscopic Constraints

High-resolution optical spectra such as those described in Section II.D give an extremely detailed picture of the ground- and excited-state potential energy surfaces in the Franck–Condon region (the Franck–Condon region is limited to the range of molecular configuration that goes from the relaxed equilibrium geometry of the ground state to that of the excited state). The measured spectra tell us that for all the linear polyenes studies so far, the equilibrium geometries of both the S_1 (1^1A_g) and S_2 (1^1B_u) states are quite close to the ground-state geometry and that the small differences primary involve changes in C=C and C—C bond lengths. The low level of vibronic activity in any low-frequency mode that could be associated with torsional motion specifically rules out significantly twisted excited states. Thus, in this case, spectroscopy defines rather than solves the problem of mechanism. The fact that the observed spectra are only consistent with there being well-defined and distinct minima for all isomers in all three of the photochemically relevant states (S_0, S_1, and S_2) tells us that we are not dealing with a barrierless process. The spectra only tell us that the barriers exist: they do not tell us how high they are nor how they are surmounted. However, this information can be derived from experiments that directly measure the effects of temperature on excited-state dynamics as is described in the next section.

2. Photophysical Constraints

2.1. S_1 Dynamics Transitions between configurations that differ by two or more spin orbitals are strictly

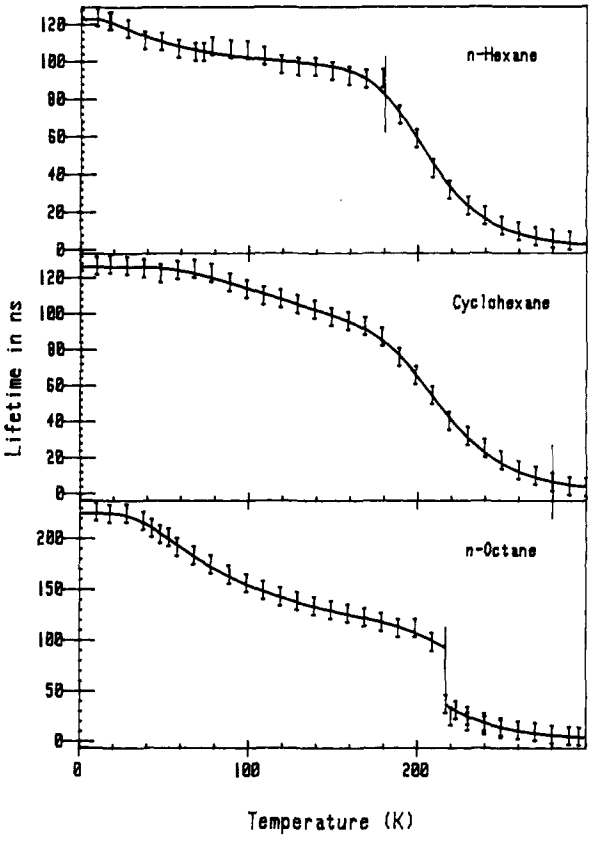

Figure 12. Fluorescence lifetime vs. temperature for octatetraene in *n*-octane (bottom), cyclohexane (middle), and *n*-hexane (top). The smooth curves are the best fit curves for a model involving a threshold process that populates a shorter lived isomer and a thermally activated decay channel.

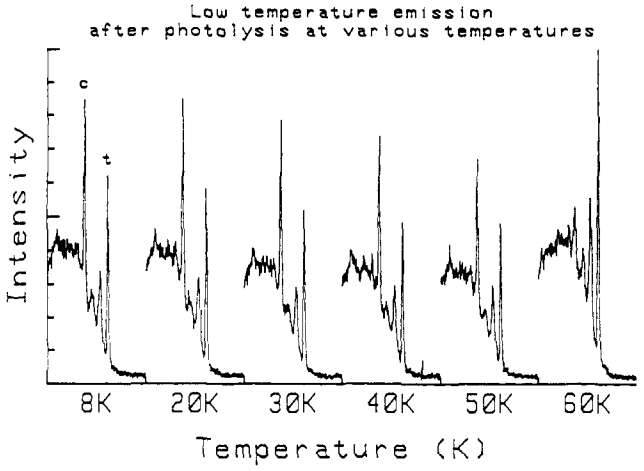

Figure 13. The 8 K origin region fluorescence spectra of a mixture of *mono-cis-* and *all-trans*-octatetraene in *n*-hexane after lamp photolyses at temperatures up to 60 K. Each scan was made at 8 K after warming the sample to the temperature indicated on the *x*-axis, irradiating (ca. 0.1 photon/molecule) and recoding. These curves were measured sequentially (left to right) for a single sample. The mono-cis origin at 28 646 cm^{-1} (labeled c) and the all-trans origin at 28 737 cm^{-1} (labeled t) are observed to maintain their relative intensities after photolyses at temperatures up to 50 K. After photolysis at 60 K, the mono-cis origin nearly vanishes and the all-trans intensity approximately doubles.

1-photon forbidden. Thus, because the configuration where two electrons are promoted from the HOMO to the LUMO is a major component of the linear polyene S_1 state, absorption intensity is weak and the lifetime for radiative decay is long even when the molecule is not strictly centrosymmetric. For example, the measured fluorescence decay time for *cis,trans*-octatetraene in 4.2 K *n*-hexane is 86 ns. Symmetry also plays a role. If the cis bond is made trans the lifetime increases to 136 ns and if the trans,trans isomer is put into a strictly centrosymmetric environment the lifetime becomes longer still (225 ns for *trans,trans*-octatetraene in *n*-octane). Much more informative, however, is the temperature dependence of these excited-state lifetimes.

The bottom panel of Figure 12 shows the fluorescence decay time of an *n*-octane solution of *trans,trans*-octatetraene measured as a function of temperature. Onsets of nonradiative decay processes are evident at approximately 50 K and, more dramatically, at approximately 220 K. In a conventional interpretation, the process at ca. 50 K would be ignored and that at ca. 220 K would be associated with trans to cis isomerization facilitated by the melting of the *n*-octane at 217 K. As appealing as this interpretation might be, it is inconsistent with the middle and upper panels of Figure 12 which show that analogous temperature dependencies are seen for *trans,trans*-octatetraene in *n*-hexane (mp 178 K) and cyclohexane (mp 280 K). The near identity of the curves measured in *n*-hexane and cyclohexane makes it clear that the process at 220 K does not depend on viscosity. A coherent and consistent interpretation of the curves in Figure 12 is the following.

The inflection at 50 K is associated with thermally activated trans to cis isomerization on the S_1 excited state surface. The existence of a thermally activated channel between *trans,trans*- and *cis,trans*-octatetraene on the S_1 potential energy surface has been established by irradiating a mixture of the cis,trans and trans,trans isomers at different temperatures.[72] At temperatures below 50 K, irradiation has little effect; above 50 K *cis,trans*-octatetraene is converted to *trans,trans*-octatetraene with nearly 100% efficiency as is seen in Figure 13. The dependence of excited-state lifetime on temperature between 50 K and 150 K, specifically the fact that it does not rapidly drop to zero with increasing temperature, proves that isomerization on the S_1 surface is indeed adiabatic; that is, both reactant and product molecules are electronically excited. The idea that the decrease in lifetime derives from thermal access to the shorter lived cis conformation is further supported by fact that, as is seen in Figure 14, effective fluorescence decay times measured for a solution of *cis,trans*-octatetraene under conditions where emission from both isomers contribute converge at ca. 50 K to the same values as those derived from measurements on a solution of the trans,trans isomer. While the implications with respect to adiabatic photochemistry are clear (as the excited cis,trans isomer is converted into the longer lived excited trans,trans isomer, there is an apparent increase in emission lifetime), as has been mentioned elsewhere,[73] the number of unknown parameters involved in the analysis of these data rules out a meaningful quantitative treatment until more detailed experimental information is available.

It is worth mentioning that the dependence of excited-state lifetime on vibronic energy that is seen for isolated diphenylbutadiene and isolated diphenylhexatriene strongly supports the notion that the low barrier to double-bond isomerization on the S_1 potential energy

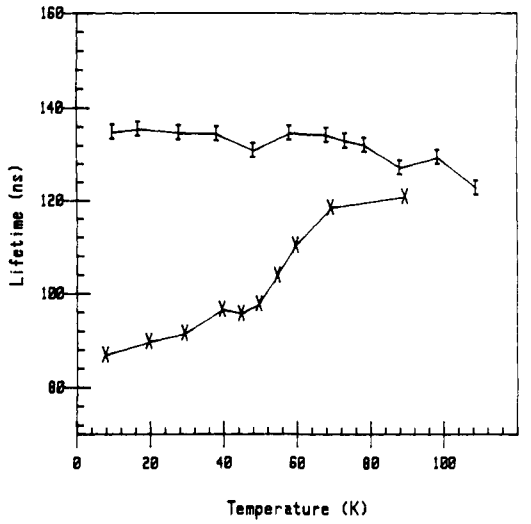

Figure 14. Apparent fluorescence lifetimes as a function of temperature for octatetraene in *n*-hexane. The points plotted in I were obtained for a solution of the trans,trans isomer; those plotted as X were measured for a solution of the cis,-trans isomer (at higher temperatures where the decay observed for selective excitation of the cis,trans isomer is no longer a single exponential, the data were fit by two decay times and the longer component plotted).

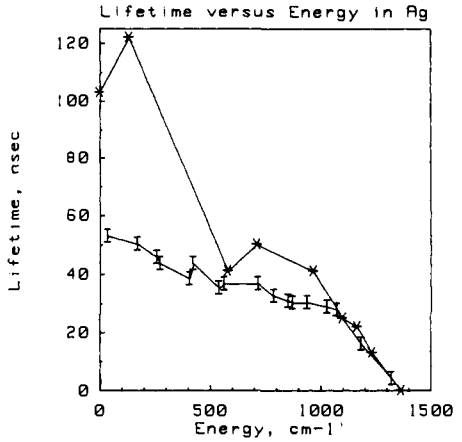

Figure 15. Fluorescence decay lifetimes as a function of excitation energy relative to the 1^1A_g–2^1A_g 0–0 for diphenylbutadiene seeded in a supersonic helium expansion. The points plotted as asterisks are for two-photon excitation and those plotted as I's are for one-photon excitation. The lines connecting the points are visual aids only.

surface reflects intrinsic properties of the linear polyene S_1 state; that is, nonbonded interactions do not make a significant contribution to the effective double-bond barrier. In the case of diphenylbutadiene seeded into a supersonic He expansion, a plot of excited-state decay time versus vibronic energy (Figure 15) shows a change in lifetime at ca. 400 cm^{-1} and the onset of an efficient nonradiative channel at ca. 1200 cm^{-1} which is analogous to the behavior of octatetraene in the condensed phase.[74-76] For two-photon excitation at the 2^1A_g 0–0, the excited-state lifetime is roughly twice as long as for one-photon excitation at the one-photon false origin. It is easy to see from simple vibronic coupling arguments that this is expected when both ground and excited states have A_g symmetry (Figure 16).[77,78] One-photon transitions are only allowed between vibronic levels whose total symmetry (electronic times vibration) with respect to inversion is opposite. Since the vibronic symmetry of the ground state is A_g (A_g symmetry electronic state times a_g symmetry vibrational state),

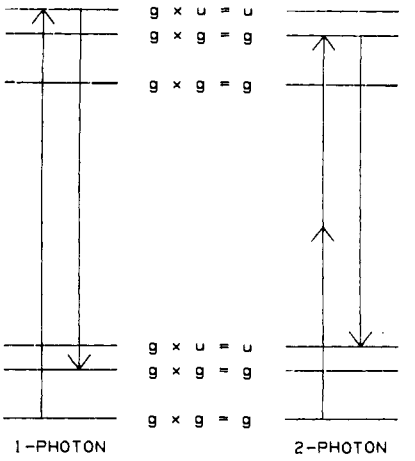

Figure 16. Selection rules are for the symmetry forbidden 1^1A_g to 2^1A_g transition for molecules initially in the zero-point level of the ground state. One-photon excitation prepares an odd-symmetry vibronic level in the excited state while two-photon excitation is to an even symmetry vibronic level. Thus, for the fluorescence from isolated molecules, the odd symmetry intensity inducing vibronic level is in the excited state for one-photon excitation and in the ground state for two-photon excitation. Because of the larger energy denominators, the two-photon allowed levels are expected to have longer radiative decay.

one-photon excitation prepares a B_u symmetry excited level (A_g symmetry electronic state times b_u symmetry vibrational state). Transition intensity for both absorption and fluorescence comes from the mixing of this excited-state vibronic level with B_u symmetry electronic states. Two-photon excitation prepares A_g symmetry excited-state levels which can then only emit to ground state levels of B_u total symmetry (A_g electronic state times b_u symmetry vibrational state). In this case transition intensity for fluorescence comes from the mixing of a ground-state vibronic level with B_u symmetry electronic states. Because the energy differences for the vibronic mixing from which the fluorescence intensity derives are smaller for one-photon excitation case (excited-state level mixes) than in the two-photon case (ground-state level mixes), fluorescence lifetimes are expected to be shorter. However, at vibronic energies above 400 cm^{-1} the lifetimes for one-photon excited levels and two-photon excited levels converge to a common value. This tells us that at this level of vibronic excitation the molecule loses its center of symmetry during the lifetime of the excited state, as would be expected for adiabatic trans to cis isomerization. The nature of the nonradiative channel that is associated with vibronic energies above 1200 cm^{-1} is not known although it is interesting that this channel is not seen in the case of isolated diphenylhexatriene.[79]

The second, and in some ways the most striking, feature of the curves in Figure 12 is the sharp decrease of S_1 lifetime with increasing temperature in the vicinity of 200 K. The profiles of lifetime versus temperature in the range 150 K to 300 K measured in *n*-hexane and cyclohexane are both well fit by a model that assumes the onset of a thermally activated decay channel with a barrier height of 4 kcal/mol. This is not the case for the abrupt change in lifetimes seen in the *n*-octane solvent for reasons that relate to symmetry rather than any significant dependence of the relevant potential energy surfaces on nonbonded interactions with the solvent. In solid *n*-octane, but not in *n*-hexane nor in cyclohexane, both the solute *and* its environment are

strictly centrosymmetric. In consequence, the low-temperature lifetime is roughly twice as long as it is for *trans,trans*-octatetraene in the noncentrosymmetric environments found in randomly ordered liquids or in solid *n*-hexane and cyclohexane. Thus, as the *n*-octane freezes forming a perfectly ordered molecular environment for the octatetraene guest molecule the intrinsic radiative decay rate discontinuously decreases as the S_1 to S_0 transition becomes strictly *symmetry* forbidden. Said another way, what is unusual about the *n*-octane solvent is that the symmetry of the local environment changes discontinuously as the solvent melts. This is not the case for *n*-hexane and cyclohexane.

The experiments on the temperature dependence of cis to trans isomerization definitively show that this process begins to compete with excited-state decay at ca. 50 K so the thermally activated process responsible for the decrease in excited-state lifetime at ca. 200 K must have other origins. Given that the lifetime associated with this channel is approximately 50 ns at 200 K, the Arrhenius activation energy for this decay channel must be between 1200 and 1800 cm^{-1} (preexponential factor 10^{11} to 10^{13} s^{-1}). This differs enough from the 3500 cm^{-1} S_2–S_1 gap to make it unlikely that this decay is associated with the S_2 state. Since the temperature at which this process begins to compete with other S_1 decay channels is the same in liquid and solid solvents, this decay channel is associated with intrinsic properties of the octatetraene potential energy surfaces; that is, it is insensitive to nonbonded perturbations. This conclusion is reinforced by the fact that an analogous dependence of S_1 lifetime on vibronic energy is seen for isolated octatetraene.[80] That a similar decrease in excited-state lifetime with S_1 vibronic energy is not seen for isolated diphenylhexatriene[79] and that the effectiveness of this channel for isolated diphenylbutadiene is greatly reduced by the introduction of buffer gas[81] are consistent with the idea that this nonradiative process is associated with coherent motion along some vibrational coordinate. At this point not enough is known to give a molecular level description of the nonradiative process that turns on at ca. 200 K, so the identification of the nonradiative process that is associated with the ca. 1500 cm^{-1} barrier remains an interesting and open question.

2.2. Photochemical Hole Burning The thermal cycling experiments described in the preceding section definitively show that at approximately 55 K thermally activated isomerization of *cis,trans*-octatetraene to the trans,trans isomer in the S_1 state begins to compete with excited state decay. Subsequent studies of the temperature dependence of excited-state decay processes for *cis,cis*-octatetraene[73] lead to a schematic view of the octatetraene S_1 potential energy surface where there is a well-defined minimum for each isomer at a geometry very similar to the ground-state equilibrium geometry and where the minimum-energy paths between these minima are quite low (Figure 17). Photochemical holeburning studies provide strong confirmation of this picture.

Even though the S_0–S_1 vibronic bands that are seen for octatetraene in low-temperature *n*-alkane crystals are extremely narrow (bandwidths are typically ca. 10 cm^{-1}), they are still very much broader than they could be. The width in cm^{-1} $\delta\bar{\nu}$ expected for the fluorescence

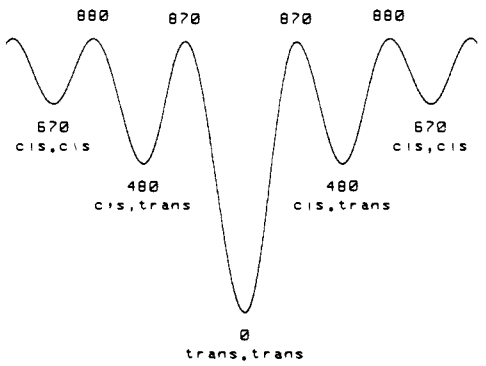

Figure 17. Schematic picture of the potential energy surface for the octatetraene 2^1A_g state. The molecular conformation at the minima and the relative energies in cm^{-1} are labeled in the figure.

origin band of an ensemble of identical molecules whose excited-state lifetime is τ is given by the lifetime-energy uncertainty relation $\delta\bar{\nu} = (2\pi C\tau)^{-1}$, where C is the velocity of light. In the particular case of octatetraene in *n*-hexane where the fluorescence lifetime at 4.2 K is 100 ns, this gives a width of only 0.000 05 cm^{-1}, which is 2×10^5 times narrower than the observed bandwidth. The fact that the observed band is so much broader than the intrinsic width derives from the fact that electronic excitation energies are distributed over a 10 cm^{-1} range by small variations in the microscopic environments of the solute molecules. That is, the observed profile is the superposition of the intrinsic 0.000 05 cm^{-1} wide profiles spread over a 10 cm^{-1} range of excitation energies. Since octatetraene can still undergo photoisomerization in these low-temperature crystals, by irradiating with extremely monochromatic laser sources this photochemistry can be limited to only those molecules whose 0.000 05 cm^{-1} wide absorption bands overlap with the laser. When these molecules are photoisomerized, they no longer contribute to the band profile which, in consequence, develops a notch called a persistent photochemical hole. This is depicted in cartoon form in Figure 18. Hole burning experiments yield two pieces of photochemically relevant information: the efficiency with which a persistent photochemical hole is burned (hole area normalized to the area of the broadened band per photon absorbed) is determined by the photochemical quantum yield, and in the low-temperature low-conversion limit, the width of the hole is determined by the excited-state lifetime.

Thus far, the application of hole burning techniques to the study of linear polyene photoisomerization in low-temperature crystals has been limited to the case of *trans,trans*-octatetraene in *n*-hexane.[82] In this case it was shown that, to within the ability to measure the widths of the very narrow holes that could be burned into the 0–0 band, they were determined by the 100-ns excited-state lifetime. The widths of photochemical holes burned into vibronic bands above the 0–0 were very much broader, reflecting the fact that the time scale for vibrational relaxation in the condensed phase is in the ps range. While the vibronic level lifetime showed no coherent trend with increasing energy, the hole burning efficiency (relative yield for photoisomerization) did, increasing by a factor of 40 as the vibronic energy exceeded 900 cm^{-1} (Figure 19). The fact that the dependence of relative photoisomerization yield on vibronic energy is well fit by an energy threshold law

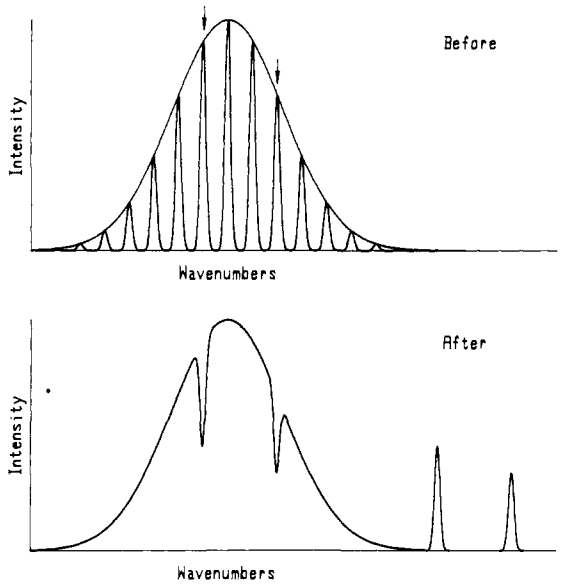

Figure 18. Photochemical hole burning. The upper curve indicates an inhomogeneously broadened absorption bond that is the superposition of contributions from molecules in different microenvironments. Irradiation with monochromatic light at the frequencies indicated selectively isomerizes only those molecules in resonance with the laser leaving persistent photochemical holes as indicated in the lower curve.

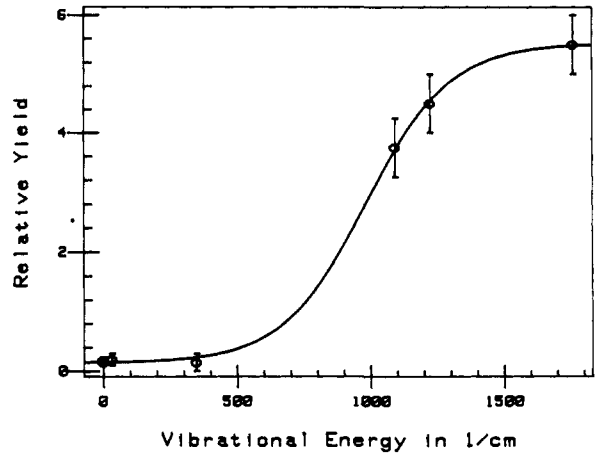

Figure 19. The efficiency of photochemical hole burning in the $1^1A_g \rightarrow 2^1A_g$ transition of *all-trans*-octatetraene in *n*-hexane at 4.2 K as a function of vibrational energy. The smooth curve is the best fit to the data by the energy gap expression, $\varphi_r = \varphi_0/(1 + e^{a(\Delta E - E)})$. The best-fit value for the energy gap ΔE is 950 ± 30 cm^{-1}.

with a threshold energy that agrees with the thermal barrier to photoisomerization on the S_1 potential energy surface derived from the dependence of excited-state decay time and isomer interconversion on temperature provides strong conformation for adiabatic photoisomerization. The potential of these kinds of studies to contribute to our understanding of photochemistry in well-defined solid-state environments is substantial: it is hoped that future work will lead to a much broader realization of this potential.

IV. Summary and Conclusions

Since the kind of low-temperature isomerization phenomena that are described in this article did provide a method for making a sample of *cis,cis*-octatetraene, something that cannot be accomplished with more traditional methods, it is even possible to claim that they have utility for synthesis. However, this is rather limited. The principal value of photochemical studies under high-resolution conditions rests in the special leverage that they give us for understanding the molecular mechanism of the very fundamental process of photoisomerization in a solvent cavity. While the correlation of vibrationally resolved spectroscopic and photochemical behavior described here has concentrated on octatetraene in solid solution, the mechanistic picture that emerges is expected to have broad applicability. In the particular case of octatetraene in an *n*-alkane crystal it is now clear that there are three channels. The fact that the molecules photoisomerize, albeit very inefficiently when excited directly to the S_1 0–0 level (as demonstrated in the hole burning studies), establishes that isomerization can take place after internal conversion on the S_0 state surface in competition with vibrational relaxation. The 40-fold increase in photoisomerization yield at liquid helium temperatures for excitation >900 cm^{-1} above the S_1 0–0 seen in the hole burning studies identifies a coherent channel that can compete with vibrational relaxation on the S_1 potential energy surface. At temperatures between 60 K and 200 K it appears that thermodynamic equilibrium with respect to the trans,trans, cis,trans, and cis,cis species is achieved within the excited-state lifetime. This identifies a third channel, important at higher temperatures, which is thermally activated isomerization on the S_1 state potential energy surface. Excitation energies of all three double bond isomers are nearly the same which means that in the S_1 state, as in the ground state, energy increases ca. 2 kcal/mol per double bond cis linkage. In consequence, between 60 K and 200 K the yields for cis,trans and cis,cis to go to trans,trans are expected to be high (certainly greater than 80%) and the yield for trans,trans to isomerize must be correspondingly low. Although it is also very clear that in the case of this unsubstituted molecule vicosity plays almost no role in the photodynamics, the situation at higher temperatures is not well understood. The unambiguous determination of the nature of the process responsible for the thermally activated decay channel responsible for the dramatic shortening of S_1 lifetime at ca. 200 K may well constitute the next significant advance in our understanding of polyene photoisomerization in a molecular cavity.

Acknowledgments. The work from my own laboratory that is described here is that of an extraordinary cohort of graduate students, undergraduate students, and postdoctoral fellows. Those that have contributed to the story told here include (in chronological order): Bruce Hudson, Ronald Christensen, Roy Auerbach, Mark Granville, John Ackerman, Judith Snow, Musharaf Hossain, Stuart Forman, Lou Ann Heimbrook, Gary Holtom, Jon Kenney, Tom Spiglanin, Paul West, Pradip Mitra, Jim Horwitz, Takao Itoh, Curtis Westerfield, Wybren Buma, Kyuseok Song, and Tom Shaler. These people gave me a story to tell; Colleen Fleming's word processing skills made the telling a pleasure. My thanks to all!

References

(1) Birge, R. R. *Biochim. Biophys. Acta* **1990**, *1016*, 293.
(2) Baughman, R. H.; Kohler, B. E.; Levy, I. J.; Spangler, C. *Synthetic Metals* **1985**, *11*, 37.

(3) (a) Norman, N.; Mathison, H. *Acta Chem. Scand.* **1961**, *15*, 1755. (b) Norman, N.; Mathison, H. *Acta Chem. Scand.* **1972**, *26*, 3913.
(4) Lide, D. R. *Tetrahedron* **1962**, *17*, 125.
(5) Ackerman, J. R.; Kohler, B. E. *J. Chem. Phys.* **1984**, *80*, 45.
(6) Ackerman, J. R.; Forman, S. A.; Hossain, M.; Kohler, B. E. *J. Chem. Phys.* **1984**, *80*, 39.
(7) Buma, W. J.; Kohler, B. E.; Song, K. *J. Chem. Phys.* **1991**, *94*, 4691.
(8) Kasha, M. *Discuss. Faraday Soc.* **1950**, *9*, 14.
(9) Havinga, V. E. *Chimia* **1962**, *16*, 145.
(10) Hudson, B. S.; Kohler, B. E. *Chem. Phys. Letts.* **1972**, *14*, 299.
(11) Schulten, K.; Karplus, M. *Chem. Phys. Letts.* **1972**, *14*, 305.
(12) Koutecky, J. *J. Chem. Phys.* **1967**, *47*, 1501.
(13) Simonetta, M.; Gianinetti, E.; Vandoni, I. *J. Chem. Phys.* **1968**, *48*, 1579.
(14) Hudson, B. S.; Kohler, B. E. *J. Chem. Phys.* **1973**, *59*, 4984.
(15) Orlandi, G.; Zerbetto, F.; Zgierski, M. Z. *Chem. Rev.* **1991**, *91*, 867.
(16) Kohler, B. E. *Carotenoids: Volume 1B*; Birkhäuser Verlag Publishers: Basel, Switzerland, 1992.
(17) Salem, L. *The Molecular Orbital Theory of Conjugated Systems*; W. A. Benjamin, Inc.: Reading, MA, 1966.
(18) Kohler, B. E. *J. Chem. Phys.* **1990**, *93*, 5838.
(19) Strickler, S. J.; Berg, R. A. *J. Chem. Phys.* **1962**, *37*, 814.
(20) Ackerman, J. R.; Huppert, D.; Kohler, B. E.; Rentzepis, P. M. *J. Chem. Phys.* **1982**, *77*, 3967.
(21) Sclar, L. A.; Hudson, B.; Peterson, M.; Diamond, J. *Biochemistry* **1977**, *16*, 813.
(22) D'Amico, K. L.; Manos, C.; Christensen, R. L. *J. Am. Chem. Soc.* **1980**, *102*, 1777.
(23) For the theory of solvent shifts, see: Basu, S. *Adv. Quantum Chem.* **1964**, *1*, 145. Amos, A. J.; Burrows, B. L. *Adv. Quantum Chem.* **1973**, *7*, 303.
(24) Hollas, J. M. *Modern Spectroscopy*, 2nd ed.; John Wiley and Sons: New York, 1992.
(25) Levy, D. H. *Annu. Rev. Phys. Chem.* **1980**, *31*, 197 and references therein.
(26) Buma, W. J.; Kohler, B. E.; Song, K. *J. Chem. Phys.* **1990**, *92*, 4622.
(27) Buma, W. J.; Kohler, B. E.; Song, K. *J. Chem. Phys.* **1991**, *94*, 6367.
(28) Buma, W. J.; Kohler, B. E.; Shaler, T. A. *J. Chem. Phys.* **1992**, *96*, 399.
(29) Buma, W. J.; Kohler, B. E.; Nuss, J. M.; Shaler, T. A.; Song, K. *J. Chem. Phys.* **1992**, *96*, 4860.
(30) Bouwman, W. G.; Jones, A. C.; Phillips, D.; Thibodeau, P.; Friel, C.; Christensen, R. L. *J. Phys. Chem.* **1990**, *94*, 7429.
(31) Petek, H.; Bell, A. J.; Christensen, R. L.; Yoshihara, K. *J. Chem. Phys.* **1992**, *96*, 2412.
(32) Granville, M. F.; Holtom, G. R.; Kohler, B. E. *J. Chem. Phys.* **1980**, *72*, 4671.
(33) The excitation energies from ref 32, 34–44 are summarized in Table I of reference 18.
(34) Granville, M. F.; Kohler, B. E.; Snow, J. B. *J. Chem. Phys.* **1981**, *75*, 3765.
(35) Snow, J. B. Unpublished result.
(36) Snyder, R.; Arvidson, E.; Foote, C.; Harrigan, L.; Christensen, R. O. *J. Am. Chem. Soc.* **1985**, *107*, 4117. The excitation energy was obtained by digitizing a photocopy of the original figure and then least-squares fitting a Gaussian to the 0–0 band.
(37) Andrews, J. R.; Hudson, B. S. *Chem. Phys. Letts.* **1978**, *57*, 600.
(38) Christensen, R. L.; Kohler, B. E. *J. Chem. Phys.* **1975**, *63*, 1837.
(39) Auerbach, R. A.; Christensen, R. L.; Granville, M. F. *J. Chem. Phys.* **1981**, *74*, 4.
(40) Simpson, J. H.; McLaughlin, L.; Smith, D. S.; Christensen, R. L. *J. Chem. Phys.* **1987**, *87*, 3360.
(41) Kohler, B. E.; Spangler, C. W.; Westerfield, C. *J. Chem. Phys.* **1988**, *89*, 5422.
(42) Heatherington, W. M. III Ph.D. Thesis, Stanford University, 1977.
(43) Westerfield, C. Ph.D. Thesis, University of California, Riverside, 1991.
(44) Horwitz, J. S.; Itoh, T.; Kohler, B. E.; Spangler, C. W. *J. Chem. Phys.* **1987**, *87*, 2433.
(45) Andersson, P. O.; Gillbro, T.; Asato, A. E.; Liu, R. S. H. *J. Luminescence* **1992**, *51*, 11.
(46) Gillbro, T.; Cogdell, R. J. *Chem. Phys. Letts.* **1989**, *158*, 312.
(47) Shreve, A. P.; Trautman, J. K.; Owens, T. G.; Albrecht, A. C. *Chem. Phys. Letts.* **1991**, *178*, 89.
(48) Hudson, B. S.; Kohler, B. E.; Schulten, K. *Excited States* **1982**, *6*, 1.
(49) Baeriswyl, D.; Campbell, D. K.; Mazumdar, S. *Conducting Polymers*; Springer: New York, 1990.
(50) Dixit, S. N.; Mazumdar, S. *Phys. Rev. B* **1984**, *29*, 1824.
(51) Soos, Z.; Ramasesha, S. *Phys. Rev. B* **1984**, *29*, 5410.
(52) Baeriswyl, D.; Maki, K. *Phys. Rev. B* **1985**, *31*, 6633.
(53) Ohmine, I.; Karplus, M.; Schulten, K. *J. Chem. Phys.* **1978**, *68*, 2298.
(54) Lennard-Jones, J. E. *Proc. R. Soc. London, Ser. A* **1937**, *158*, 280.
(55) Dixit, S. N.; Guo, D.; Mazumdar, S. *Phys. Rev. B* **1991**, 6781.
(56) Gottfried, D. S.; Steffen, M. A.; Boxer, S. A. *Science* **1991**, *252*, 662.
(57) Gottfried, D. S.; Steffen, M. A.; Boxer, S. A. *Biochim. Biophys. Acta* **1991**, *1059*, 76.
(58) van Beek, J. B.; Kajzar, F.; Albrecht, A. C. *Chem. Phys.* **1992**, *161*, 299. van Beek, J. B.; Kajzar, F.; Albrecht, A. C. *J. Chem. Phys.* **1991**, *95*, 6400.
(59) Birnbaum, D.; Kohler, B. E.; Spangler, C. W. *J. Chem. Phys.* **1991**, *94*, 1684.
(60) Kohler, B. E.; Spangler, C. W.; Westerfield, C. *J. Chem. Phys.* **1991**, *94*, 908.
(61) Sun, Y.-P.; Sears, D. F., Jr.; Saltiel, J. *Anal. Chem.* **1987**, *59*, 2515.
(62) Granville, M. F.; Holtom, G. R.; Kohler, B. E. *Proc. Nat. Acad. Sci. U.S.A.* **1980**, *77*, 31.
(63) Kohler, B. E.; Spiglanin, T. A. *J. Chem. Phys.* **1984**, *80*, 3091.
(64) Ackerman, J. R. Ph.D. Thesis, Wesleyan University, Middletown, CT, 1983.
(65) Ackerman, J. R.; Kohler, B. E.; Wu, K. T. *Photoreaktive Festokörper*; M. Wahl-Verlag: Karlsruhe, 1984; p 121.
(66) Data, P.; Goldfarb, T.; Boikes, R. *J. Am. Chem. Soc.* **1969**, *91*, 5429.
(67) Kohler, B. E.; West, P. *J. Chem. Phys.* **1983**, *79*, 583.
(68) Kohler, B. E. *Photochemistry and Photobiology: Proceedings of the International Conference*; Harwood Academic Publishers: Chur, Switzerland, 1983.
(69) Hossain, M.; Kohler, B. E.; West, P. *J. Phys. Chem.* **1982**, *86*, 4918.
(70) Squillacote, M. E.; Sheridan, R. S.; Chapman, O. L.; Anet, F. A. L. *J. Am. Chem. Soc.* **1979**, *101*, 3657.
(71) Ackerman, J. R.; Forman, S. A.; Katz, L.; Kohler, B. E.; Wu, K. T. *J. Chem. Phys.* **1984**, *81*, 3387.
(72) Ackerman, J. R.; Kohler, B. E. *J. Am. Chem. Soc.* **1984**, *106*, 3681.
(73) Kohler, B. E.; Mitra, P.; West, P. *J. Chem. Phys.* **1986**, *85*, 4436.
(74) Heimbrook, L.; Kohler, B. E.; Spiglanin, T. A. *Proc. Nat. Acad. Sci. U.S.A.* **1983**, *80*, 4580.
(75) Felker, P. M.; Zewail, A. H. *Chem. Phys. Lett.* **1984**, *108*, 303.
(76) Horwitz, J. S.; Kohler, B. E.; Spiglanin, T. A. *J. Chem. Phys.* **1985**, *83*, 2186.
(77) Horwitz, J. S.; Kohler, B. E.; Spiglanin, T. A. *J. Phys.* **1985**, *C7*, 381.
(78) Horwitz, J. S.; Itoh, T.; Kohler, B. E.; Spiglanin, T. A. *SPIE Proc.* **1989**, *1057*, 72.
(79) Kohler, B. E.; Spiglanin, T. A. *J. Chem. Phys.* **1984**, *80*, 5465.
(80) Buma, W. J.; Kohler, B. E.; Shaler, T. A. *J. Chem. Phys.* **1992**, *96*, 399.
(81) Itoh, T.; Kohler, B. E. *J. Phys. Chem.* **1988**, *92*, 1807.
(82) Adamson, G.; Gradl, G.; Kohler, B. E. *J. Chem. Phys.* **1989**, *90*, 3038.